ICES Journal of Marine Science

ICES Journal of Marine Science (2022), 79(1), 22–33. https://doi.org/10.1093/icesjms/fsab224

Downloaded from https://academic.oup.com/icesjms/article/79/1/22/6453070 by Institute of Marine Research user on 17 February 2022

Original Article

Modelling chemical releases from fish farms: impact zones, dissolution time, and exposure probability

Pål Næverlid Sævik*, Ann-Lisbeth Agnalt, Ole Bent Samuelsen, and Mari Myksvoll

Institute of Marine Research, P.B. 1870 Nordnes, 5817 Bergen, Norway

*Corresponding author: tel:+47 55 23 85 00; e-mail: paal.naeverlid.saevik@hi.no

Sævik, P. N., Agnalt, A.L., Samuelsen, O. B., and Myksvoll, M. Modelling chemical releases from fish farms: impact zones, dissolution time, and exposure probability. – ICES Journal of Marine Science, 79: 22–33.

Received 28 April 2021; revised 8 October 2021; accepted 21 October 2021; advance access publication 5 December 2021.

Tarpaulin bath treatments are used in open net-pen finfish aquaculture to combat parasitic infections, in particular sea lice. After treatment, the toxic wastewater is released directly into the ocean, potentially harming non-target species in the vicinity. We model the dispersion of wastewater chemicals using a high-resolution numerical ocean model. The results are used to estimate the impact area, impact range, dissolution time, and exposure probability for chemicals of arbitrary toxicity. The study area is a fish-farming intensive region on the Norwegian western coast. Simulations are performed at 61 different release dates, each on 16 locations. In our base case where the chemical is toxic at 1% of the treatment concentration, the release of a 16000 m^3 wastewater plume traverses a median distance of 1.9 km before being completely dissolved. The median impacted area is 0.9 km^2 and the median dissolution time is 6.8 hours. These figures increase to 5.9 km, 7.0 km^2, and 21 hours, respectively, if the chemical is toxic at 0.1 % of the treatment concentration. Locations within fjords have slower dissolution rates and larger impact zones compared to exposed locations off the coast, especially during summer.

Keywords: aquaculture, bath treatment, dispersion, numerical ocean model, particle tracking, ROMS, sea lice, wastewater.

Introduction

Cage-based marine aquaculture of salmonids is a growing form of food production. The industry produced 2.79 million tons globally in 2018, worth 19.7 billion USD (FAO, 2020). Of these, 1.4 million tons were produced in Norway and 0.9 million tons in Chile. The production consists primarily of Atlantic Salmon (*Salmo salar*) and to a lesser degree rainbow trout (*Oncorhynchus mykiss*). A major challenge faced by the industry is parasitic infections by various species of sea lice. In Europe and eastern North America, the species *Lepeophtheirus salmonis* has caused the most concern (Johnson *et al.*, 2004; Torrissen *et al.*, 2013; Taranger *et al.*, 2015; Forseth *et al.*, 2017), while *Caligus rogercresseyi* infestations has plagued fish farmers on the pacific coast of South America (Hamilton-West *et al.*, 2012).

Sea lice are ectoparasitic copepods that feed on the skin, blood, and mucus of its host (Kabata, 1974; Wootten *et al.*, 1982). If uncontrolled, the parasite may multiply in large numbers in aquaculture-dense areas due to the abundant availability of hosts (Heuch and Mo, 2001; Bergh, 2007), causing significant economic losses (Costello, 2009; Kragesteen *et al.*, 2019). Additionally, elevated parasite abundance has a negative influence on the wild population of Brown trout (*Salmo trutta*) (Skaala *et al.*, 2014), as well as young wild Atlantic salmon who migrate from their river of origin towards the ocean during spring season (Hvidsten *et al.*, 2007; Johnsen *et al.*, 2020). To protect wild salmonid populations, Norwegian fish farmers are required by law to keep the number of adult female lice per fish below 0.2 in the spring season, and below 0.5 during the rest of the year (Lovdata, 2018).

One conventional method for reducing sea lice levels in open net pens is in-situ bath treatments using anti sea-lice pharmaceuticals. In this procedure, a fish cage under treatment is enclosed by a tarpaulin, and the therapeutant is added. After treatment, the tarpaulin is removed, and the treatment water is transported away

© The Author(s) 2021. Published by Oxford University Press on behalf of International Council for the Exploration of the Sea. This is an Open Access article distributed under the terms of the Creative Commons Attribution License (https://creativecommons.org/licenses/by/4.0/), which permits unrestricted reuse, distribution, and reproduction in any medium, provided the original work is properly cited.

by ocean currents. Commonly used bath treatment chemicals contain either deltamethrin, azamethiphos, or hydrogen peroxide as active ingredients. While the treatment procedures are designed to kill sea lice on farmed fish, the released wastewater may potentially reach sensitive non-target organisms in the vicinity before being diluted to environmentally benign concentrations.

To protect marine wildlife, it is important to know how far from the release site one can expect to find toxic concentrations. There has been attempts to answer this question using field studies (Ernst *et al.*, 2014; Andersen and Hagen, 2016; Fagereng, 2016). Unfortunately, field studies are not particularly well suited for this purpose. The first problem is the heterogeneity of the turbulent dilution process, which makes measurements highly sensitive to sampling location and depth. The second problem is that only a relatively small number of locations can be sampled simultaneously, making it difficult to obtain a clear picture of the plume size. The third problem is that field studies of the required scale are expensive, and one can not afford many repetitions of the same experiment. Thus, it is difficult to know whether the estimated impact area is representative for releases occurring at other times or locations. Visible dye as used by Ernst *et al.* (2014) can alleviate some of these problems, but only if the main part of the plume stays close to the surface.

In the current research, we use a numerical ocean model to simulate the release and subsequent dilution of wastewater from fish farm tarpaulin operations. This allows us to monitor multiple virtual chemical releases in full three-dimensions over a long time period and obtain a complete overview over the resulting impact zones. The ocean model have previously been used in a multitude of applications in Norwegian fjords, and has shown good agreement with observational data (Asplin *et al.*, 2020; Dalsøren *et al.*, 2020).

While scenario-specific simulations of bath treatments have been performed previously (Refseth *et al.*, 2016, 2019; Parsons *et al.*, 2020), these studies are limited in scope, and not designed to infer general statements about the expected size of the impact zones for arbitrary types of chemicals and release volumes. In the current research, we develop a statistical model using data from the numerical simulations, to estimate the sensitivity of the impact zones and plume dilution rates with respect to chemical toxicity, release concentration, location, and time of release. We also quantify how fast the exposure probability declines with the distance from the release site.

Methods

Study area

The chosen study area is the western coast of Norway between latitudes 59.5 °N and 60.5 °N. The region has two major fjord systems, Hardangerfjorden and Bjørnafjorden, which are connected to coastal water through multiple fjord mouths and inlets. The topography of the area is complex, consisting of several islands, fjords, narrows, and bays. Off the coast, currents are dominated by the Norwegian coastal current, which originates in the Baltic Sea and flows northward along the Norwegian coastline. Circulation patterns within the fjords are driven by tides, wind, and freshwater runoff from the surrounding rivers. The mean tidal range is small (∼1 m). Strong currents occur episodically in the upper ∼10 m, generated by periods of strong winds. A brackish layer generates shallow (∼5 m) outflows in periods with strong stratification close to the surface (Asplin *et al.*, 2014; Johnsen *et al.*, 2014).

Due to intensive aquaculture activity, the region has long experienced elevated levels of sea lice. Tarpaulin bath treatments have been used frequently to combat the problem. Of the 9433 registered bath treatments in Norway from 2012 to 2020, 1870 were executed at farms within our study area (www.barentswatch.no). At the beginning of the year 2021, the region contained 145 marine commercial fish farming sites. In the current research, we have simulated releases from a representative sample of 16 locations (Figure 1). These include both exposed and sheltered locations on the outer islands, sites in the outer and inner parts of the fjords, and sounds/narrows where the current circulation patterns are strongly constrained by the topography.

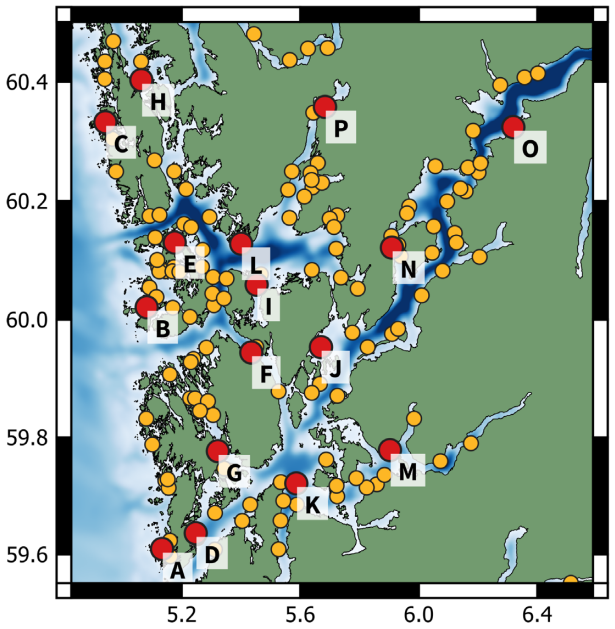

Figure 1. Map of commercial marine salmonid fish farm locations within the study area. Red labelled dots indicate the position of the 16 farms used as release points in the simulations.

Hydrodynamic model

The Regional Ocean Modelling System (ROMS) is used to simulate the fjord currents (Shchepetkin and McWilliams, 2005). The model setup is a horizontally refined version of NorKyst800 (Albretsen *et al.*, 2011), covering the study area at a horizontal resolution of 160 m × 160 m and a vertical resolution of 35 terrain-following generalized sigma coordinate levels. The original NorKyst800 model, which covers the Norwegian coast at 800 m × 800 m resolution, is used as boundary conditions for the refined subgrid. The model setup has been validated against a wide range of hydrodynamic measurements, and has been demonstrated to simulate realistic currents both within fjords and along the coast (Asplin *et al.*, 2020; Dalsøren *et al.*, 2020).

Atmospheric fields are provided from AROME MetCoOp (Meteorological Co-operation on Operational Numerical Weather Prediction) 2.5 km, the main forecasting system at the Norwegian Meteorological Institute (Müller *et al.*, 2017). Daily river flow rates are included in the simulations and based on estimates from the Norwegian Water Resources and Energy Directorate (NVE) through their updated data series from all catchment areas in Norway (https://nve.no). These data series use measured water flows to estimate the total runoff along the coastline within each catchment area.

Downloaded from https://academic.oup.com/icesjms/article/79/1/22/6453070 by Institute of Marine Research user on 17 February 2022

Dispersion model

To model dispersion of chemicals, the Lagrangian Advection and Diffusion Model (Ladim) particle tracking software is used (https://github.com/bjornaa/ladim, version 1.1). Hourly ocean currents from ROMS are used as forcing, with linear interpolation for intermediate time steps. A single release is represented by 100000 particles, initially contained within a volume of 40 m × 40 m × 10 m. This is representative for the volume of a common large-class open net pen under a tarpaulin-based delousing operation, which may vary depending on the cage design and delousing technique (Volent *et al.*, 2017). The particles are transported passively with the flow, both horizontally and vertically.

The main Ladim code base does not include vertical flow and heterogeneous turbulence, which is important to model chemical dispersion rates correctly. These features were implemented as a separate plugin module, available at https://github.com/pnsaevik/ladim_plugins (version 1.5.8). The plugin also includes modifications to the current velocity interpolation scheme and the land collision treatment, to avoid artificial concentration buildup near shores. We now briefly describe each of these improvements and refer to the source code for additional details.

As previously stated, we use velocity currents from ROMS, which are provided on a staggered Arakawa C-grid (Arakawa and Lamb, 1977). In the main Ladim code base, velocities are bilinearly interpolated, whereas the new plugin interpolates currents as in Döös *et al.* (2013) to keep the interpolated divergence consistent with the underlying numerical divergence. This eliminates one source of artificial particle clustering. Furthermore, vertical velocity is computed from the horizontal divergence and used to advect particles in the vertical direction. In the horizontal direction, particles are advected using a Runge–Kutta 4th order scheme, which reduces the probability that a particle ends up on land. If a land collision should happen nevertheless, the particle is repositioned randomly within the grid cell it originated from.

Heterogeneous turbulent mixing is modelled as a stochastic differential equation (Gräwe, 2011), and solved numerically using the scheme of LaBolle *et al.* (2000). This scheme entirely avoids artificial particle clustering for heterogeneous mixing profiles. In the horizontal direction, turbulent mixing is computed using the formulation of Smagorinsky (1963), in the form given by Kantha and Clayson (2000), Equation (1.17.6). In the vertical direction, turbulent mixing is taken directly from ROMS, which uses the Generic Length Scale model to compute the mixing coefficient (Umlauf and Burchard, 2003). For numerical stability reasons, vertical mixing is sampled at 5 m intervals and capped at a maximal value of 0.01 m^2/s.

The dispersed particle field was converted to a continuous concentration field using a standard box counting approach, where the domain of interest was divided into blocks of 100 m × 100 m in the horizontal plane and 1 m in the vertical direction. The particle concentration was computed by dividing the number of particles by the volume of the block. The normalized concentration is the particle concentration divided by the initial particle concentration inside the fish cage (6.25 particles per m^3). The actual chemical concentration is the normalized concentration times the initial release concentration.

We performed 61 releases for each of the 16 locations, one every sixth day from January 4, 2020 to December 29, 2020, all starting at 12:00. The particles were tracked for 48 hours. This allowed the plume to be completely dissolved within the simulation period, with a few exceptions.

Toxicity threshold

Previously we have used the term "plume" in a loose sense. We now define the wastewater plume more precisely as the portion of the ocean where the normalized concentration of the bath treatment chemical exceeds a pre-defined toxicity threshold. In other words, the plume boundary is a pre-defined concentration contour level. The plume is considered dissolved if the normalized concentration is below the toxicity threshold everywhere. Furthermore, we define the impact zone as the region swept by the plume during its lifetime. This includes any location which has experienced concentrations beyond the toxicity threshold at any point during the simulation, anywhere within the water column.

There is not a single unique way to determine the toxicity threshold, as the harmful potential of a chemical varies among species and may increase gradually with concentration. One strategy is to use the LC_{50} value (concentration that kills half of the organisms) of the most sensitive species in the vicinity, converted to normalized concentration units. Values such as NOEC (no observed effect concentrations) or LC_5 (concentration that kills 5 % of the organisms) can be used if a more conservative approach is desired.

Table 1 lists LC_{50} values for some non-target species relevant to Norwegian coastal waters, given an exposure time of 1 hour. Toxicity data with respect to other species and endpoints can be found, for instance, in Refseth *et al.* (2016) and Urbina *et al.* (2019). In the current work, we consider three explicit toxicity thresholds: 0.1, 0.01, and 0.001. Estimates for intermediate toxicity thresholds can be obtained by interpolation.

When simulation results are compared with actual chemical releases, one should also take the release volume into account. Halving the release volume will have an effect similar to halving the release concentration, except in the vicinity of the fish farm. This is because the plume is initially small and will expand to twice its size within a relatively short amount of time. One can account for varying release volumes by using the following definition of the toxicity threshold,

$$\text{Toxicity threshold} = \frac{\text{Reference volume}}{\text{Release volume}} \times \frac{\text{Harmful concentration}}{\text{Release concentration}} \quad (1)$$

where "harmful concentration" could be LC_{50} or any other relevant endpoint, and "reference volume" is the release volume used in our simulations (16000 m^3).

Outcome parameters

For each simulated chemical release, we computed four different outcome parameters related to plume exposure. Here we define each outcome parameter in order and briefly discuss their ecological significance.

The *impact area* is simply the area of the impact zone. Impact area is relevant, for instance, if the sensitive species under consideration is plentiful and can reproduce relatively quickly. If the typical impact area is small compared to the species' habitat, occasional plume exposures may be of little concern.

The *impact range* is the horizontal distance from the release point to the farthest edge of the plume during its lifetime. A sensitive species can be considered relatively safe from exposure if the typical impact range is shorter than the distance between its habitat and the release point.

The *dissolution time* is the time elapsed from the tarpaulin is released until the plume is completely dissolved, i.e. the normalized concentration has fallen below the toxicity threshold everywhere.

Downloaded from https://academic.oup.com/icesjms/article/79/1/22/6453070 by Institute of Marine Research user on 17 February 2022

Table 1. LC_{50} values for a selected number of species with respect to hydrogen peroxide (H_2O_2), deltamethrin (Deltam.), and azamethiphos (Azam.).

Species (life stage)	Chemical	LC_{50} (g / L)	LC_{50} (normalized)	Source
Calanus spp. (CV)	H_2O_2	7.7×10^{-2}	5.1×10^{-2}	(Escobar-Lux *et al.*, 2019)
Calanus spp. (adult)	H_2O_2	3.1×10^{-2}	2.1×10^{-2}	(Escobar-Lux *et al.*, 2019)
Homarus gammarus (stg.I)	Deltam.	2.6×10^{-9}	1.3×10^{-3}	(Parsons *et al.*, 2020)
Homarus gammarus (stg.I)	Azam.	4.3×10^{-5}	4.3×10^{-1}	(Parsons *et al.*, 2020)
Homarus gammarus (stg.II)	Deltam.	2.9×10^{-9}	1.5×10^{-3}	(Parsons *et al.*, 2020)
Homarus gammarus (stg.II)	Azam.	2.1×10^{-5}	2.1×10^{-1}	(Parsons *et al.*, 2020)
Saccharina latissima (juvenile)	H_2O_2	8.1×10^{-2}	5.4×10^{-2}	(Haugland *et al.*, 2019)
Meganyctiphanes norvegicus	H_2O_2	4.9×10^{-3}	3.3×10^{-3}	(Escobar-Lux and Samuelsen, 2020)
Palaemon elegans	Deltam.	1.2×10^{-7}	6.0×10^{-2}	(Brokke, 2015)
Praunus flexuosus	Deltam.	1.1×10^{-7}	5.5×10^{-2}	(Brokke, 2015)
Ophryotrocha spp.	H_2O_2	6.4×10^{-2}	4.3×10^{-2}	(Fang *et al.*, 2018)

Exposure time is 1 hour plus a recovery period. Normalized concentrations are relative to standard treatment concentrations (Jansen, 2018), which is 1.5 g/L for hydrogen peroxide, 2 μg/L for deltamethrin, and 100 μg/L for azamethiphos.

This is an upper limit to exposure time, while most organism–plume encounters will be of significantly shorter duration. Non-target species that are robust to short chemical exposures are also relatively unharmed by chemical releases with a short dissolution time.

The *exposure probability* is the probability of being exposed to the wastewater plume at distance D from the release point. To compute exposure probability, we first created a set of concentric, donut-shaped regions around the release point, each having a width of 1 km. Within each region, the exposure probability was defined as the impact area divided by the total ocean area.

Statistical regression model

We performed a series of regression analyses to estimate the effect of input variables on the four outcome parameters defined above. We used the same type of model equation for impact area, impact range, and dissolution time, while exposure probability is modelled by a second type of equation. Model assumptions (normality, homoscedasticity, etc.) were verified by plotting residuals vs. fitted values and vs. each covariate, and by quantile-quantile plots. Statistical significance of each covariate was assessed by dropping individual variables and comparing Akaike Information Criterion (AIC) values. We also computed the change in Pearson correlation coefficient (R^2) and root mean squared error for each covariate exclusion, as a measure of their explanatory power.

Covariates for impact area (*IA*, continuous, in m), impact range (*IR*, continuous, in m), and dissolution time (*DT*, continuous, in s) are the toxicity threshold (C, categorical with levels 0.1, 0.01 [reference] and 0.001), the ocean current speed at 5 m depth (U, continuous, in m/s), time of the year (T, in Julian days), and location (L, categorical with 16 levels, deviance contrast coding). The outcome parameters were $\log_{10}$ transformed, both to normalize the data and because data exploration indicated a multiplicative dependence on the covariates. The only transformed covariate is T, which is spline smoothed. The model equation is

$$\log_{10}\mu \;=\; \alpha + \beta_C C + \beta_U U + \beta_T s\,(T) + \beta_L L \qquad (2)$$

where μ represents the expectation value of any of the outcome parameters, s is a 4-knot cyclic spline smoother, α is the intercept, and $\{\beta_i\}$ are the regression coefficients, some of which are multi-valued (i.e. those belonging to categorical or spline-smoothed covariates).

Covariates for exposure probability (*EP*, continuous between 0 and 1) are the same as in Equation (2), with an additional covariate: distance from release location (D, continuous, in km). Interaction terms between D and the other covariates are included. A logistic model was used for the outcome parameter, with model equation

$$\begin{aligned}\text{logit EP} \;=\; & \alpha + \beta_C C + \beta_U U + \beta_T s\,(T) + \beta_L L \\ & + \mathrm{D} \times (\beta_D + \beta_{DC} C + \beta_{DU} U + \beta_{DT} s\,(T) + \beta_{DL} L)\end{aligned} \qquad (3)$$

The model is fitted using sea cells only, i.e. we estimate the probability of a sea cell at a certain distance being hit by the plume. Each cell is treated as an independent observation, which is not strictly true for cells in close proximity. Consequently, the confidence intervals produced by the regression are too narrow, and we do not report them in the paper. The estimated regression coefficients are still unbiased since the dataset is produced by a balanced design.

To use Equations (2) and (3) for predictions, coefficients related to location and time can be set to zero if an average value is desired. For toxicity thresholds other than the reference thresholds, interpolation on a log scale is recommended. If the toxicity threshold C is between 0.1 and 0.01, one could set $\beta_C^{[0.001]} = 0$ and $\beta_C^{[0.1]} = 2 + \log_{10} C$, where the superscript of β_C indicate the factor level. If the toxicity threshold is between 0.01 and 0.001, we have $\beta_C^{[0.1]} = 0$ and $\beta_C^{[0.001]} = -2 - \log_{10} C$.

All statistical analyses were conducted in R Studio Elderflower (RStudio Team, 2019). Figures were either produced in Python 3 using matplotlib version 3.2.2 (Hunter, 2007) and holoviews version 1.13.3 (Rudiger *et al.*, 2020), or in R Studio using ggplot2 version 3.3.2 (Wickham, 2016) and ggmap version 3.0.0 (Kahle and Wickham, 2013).

Results

Model validation

Quantile-quantile plots and residual distribution plots generated from the linear regression model indicated no problems except for a somewhat fat-tailed residual distribution outside of 2 *SD*. In other words, the regression model may underpredict the occurrence of rare outcomes. Analysis of AIC values showed that all covariates and interaction terms were significant. The R^2 correlation coeffi-

Downloaded from https://academic.oup.com/icesjms/article/79/1/22/6453070 by Institute of Marine Research user on 17 February 2022

Table 2. Root mean squared error for the models defined by Equation (2) including all covariates (bottom row), compared with models where a single covariate is removed.

Covariate removed	Impact area	Impact range	Dissolution time
C	0.951	0.615	0.622
L	0.288	0.265	0.235
T	0.249	0.237	0.212
U	0.238	0.237	0.215
(None)	0.238	0.234	0.198

Covariates are *C* (toxicity threshold), *L* (location), *T* (release time), and *U* (ocean current speed at 5 m depth).

cients of the regression models were 0.94 for impact area, 0.86 for impact range, and 0.91 for dissolution time.

Impact area, impact range, and dissolution time

The impact area, impact range, and dissolution time are all very sensitive to the toxicity threshold, which explains most of the variation in the dataset (Table 2). The remaining covariates show significant effects as well, but they do only slightly improve the predictive power of the regression. In other words, there is a large residual variation caused by shifting current patterns in the region around the farm, which are not predictable from simple statistics. As an example of the variation seen in the simulation data, Figure 2 features three simulated releases from the same farm within the same time of year, with widely different impact ranges.

The median impact area was 0.04 km^2, 0.90 km^2, and 6.99 km^2 for toxicity thresholds of 0.1, 0.01, and 0.001, respectively (Table 3). Compared with the reference toxicity threshold of 0.01, the mean impact area increases by a factor of 8.0 if the threshold is 0.001 and reduces by a factor of 21.4 if the threshold is 0.1 (Table 4). Impact area increases by only 1 % if the local current speed at 5 m depth increases by 0.1 m/s. The magnitudes of location and release time effects (standard deviation across possible values) correspond to an impact area change of 48% and 19%, respectively. Figure 3 illustrates the effect of location for each release site, while Figure 4 plots the effect of time. Note that the trends shown in Figure 4 may be specific to the year 2020, as interannual variation was not a part of this study. The residual standard deviation is 0.24, which corresponds to an impact area change of 73 % (Table 2).

The median impact range was 0.25 km, 1.90 km, and 5.87 km for toxicity thresholds of 0.1, 0.01, and 0.001, respectively (Table 3). Compared with the reference toxicity threshold of 0.01, the mean impact range increases by a factor of 3.1 if the threshold is 0.001 and reduces by a factor of 7.6 if the threshold is 0.1 (Table 4). Impact range increases by 14% if the local current speed at 5 m depth increases by 0.1 m/s. The magnitudes of location and release time effects (standard deviation across possible values) correspond to a change of impact range by 35 % and 9 %, respectively. The residual standard deviation is 0.23, which corresponds to 71 % change of impact range (Table 2).

The median dissolution time was 0.83 hr, 6.83 hr, and 21.0 hr for toxicity thresholds of 0.1, 0.01, and 0.001, respectively (Table 3). The plume growth phase was revealed to be about half as long as the shrinkage phase, but there are large individual differences (Figure 5). The linear regression model predicts an increase in mean dissolution time by 33 % if the local current speed at 5 m depth decreases by 0.1 m/s (Table 4). Compared with the reference toxicity threshold of 0.01, the mean impact range increases by a factor of 3.1 if the threshold is 0.001 and reduces by a factor of 8.5 if the threshold is 0.1. The magnitudes of location and release time effects (standard deviation across possible values) correspond to a change in dissolution time by 35 % and 20 %, respectively. The residual standard deviation is 0.20, which corresponds to a change of dissolution time by 58 % (Table 2).

Exposure probability

Estimated coefficients for the exposure probability model given by Equation (3) are shown in Table 5. The exposure probability declines exponentially with distance, with a decline rate highly dependent on the toxicity threshold (Figure 6). For $C = 0.1$, the exposure probability is estimated by the model to be 10 % at 0.1 km, 1 % at 0.6 km, and 0.1 % at 1.1 km. For $C = 0.01$, the probability is estimated to 10 % at 1.1 km, 1 % at 2.7 km, and 0.1 % at 4.2 km. For $C = 0.001$, the probability is estimated to 10 % at 3.4 km, 1 % at 6.8 km, and 0.1 % at 10.0 km. Figure 7 shows an overlay of impact zones for all simulated release times and locations, which gives a visual impression of the exposure probability and its spatial variation.

It may be surprising that the exposure probability is small at distances comparable to the median impact range. The reason is that exposure probability represents a randomly chosen direction from the farm. In contrast, the impact range is the distance from the farm to the farthest edge of the impact zone, which is not a randomly chosen direction.

The effects of location and time of year on exposure probability are statistically significant, but of smaller magnitude compared with the toxicity threshold (Figure 8). For instance, the exposure probability for $C = 0.01$ at 2 km distance from Farm C (highly exposed location) equals the exposure probability 3.1 km from Farm P (highly sheltered location). Time of year is somewhat less important: Wintertime exposure probability for $C = 0.01$ at 2 km distance equals the summertime exposure probability at 2.4 km distance.

Note that exposure probability as defined in this paper only includes the horizontal direction. To complement this, we also computed the maximal depth penetration of the simulated wastewater plumes for different toxicity thresholds (Figure 9). When $C = 0.1$, 90 % of the simulated wastewater plumes stay within the upper 10 m for the entire simulation. For $C = 0.01$ and $C = 0.001$, 90 % of the simulated wastewater plumes stay within the upper 13 m and 18 m, respectively. The plumes are more quickly dissolved in the upper 5 m, due to stronger turbulent mixing rates near the surface.

Discussion

Relative importance of covariates

Toxicity threshold is the most influential covariate, and the only covariate that dominates over residual variation. The strong dependence on toxicity threshold is expected, as we investigated a wide range of values spanning three orders of magnitude. The entire range is relevant since both the low and high end of the range are encountered in management applications. Even though the strong effect of toxicity threshold may seem obvious, regulations do not necessarily take this effect into account. For instance, Norwegian authorities do not allow tarpaulin bath treatments within 500 m of officially recognized shrimp fields and cod spawning grounds, regardless of the release volume, concentration, or type of chemical

Downloaded from https://academic.oup.com/icesjms/article/79/1/22/6453070 by Institute of Marine Research user on 17 February 2022

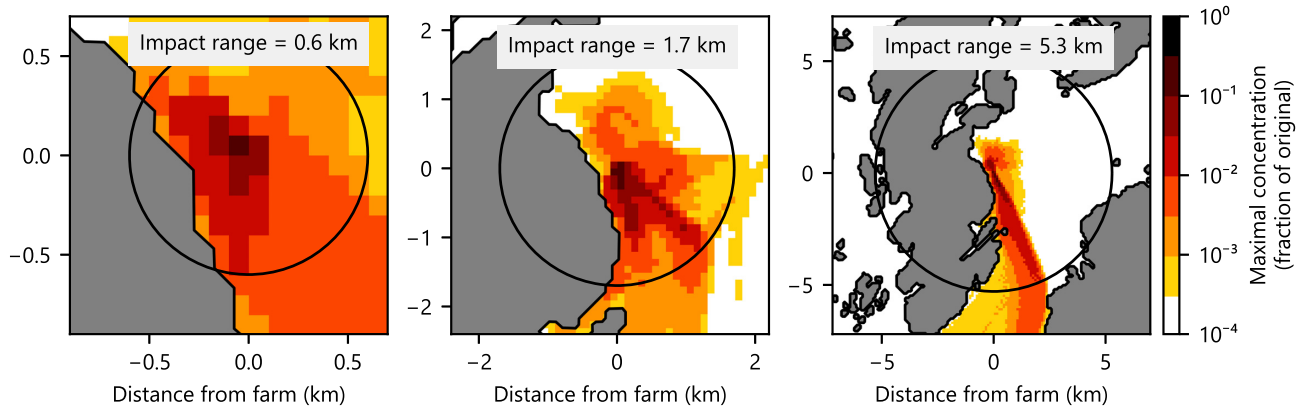

Figure 2. Simulation results for Farm D at three different release times in June and July, demonstrating large variation in impact range. Note the different spatial scales from left to right. Colours indicate the largest recorded concentration within the water column over the course of the simulation. Black circles represent the impact range for a toxicity threshold of 0.01.

Table 3. Median values for impact area, impact range, and dissolution time, grouped by the toxicity threshold value.

Toxicity threshold	Impact area (km)	Impact range (km)	Dissolution time (hr)
0.1	0.04 [0.03, 0.07]	0.25 [0.16, 0.43]	0.83 [0.50, 1.33]
0.01	0.90 [0.57, 1.40]	1.90 [1.26, 2.85]	6.83 [4.50, 10.50]
0.001	6.99 [4.90, 10.67]	5.87 [4.12, 8.29]	21.00 [14.15, 31.27]

Values in square brackets are the first and third quartiles.

Table 4. Regression coefficients for the models defined by Equation (2), with covariates U (ocean current speed at 5 m depth, in m/s), C (toxicity threshold, relative to release concentration), L (location, 16 levels), and T (time, 4-knot cyclic spline).

Covariate	$\log_{10} IA$	$\log_{10} IR$	$\log_{10} DT$
(Intercept)	5.94 (0.010)	3.22 (0.009)	4.50 (0.008)
U	0.06 (0.066)	0.56 (0.065)	− 1.25 (0.055)
C[0.001]	0.90 (0.011)	0.49 (0.011)	0.49 (0.009)
C[0.1]	− 1.33 (0.011)	− 0.88 (0.011)	− 0.93 (0.009)
L (magnitude)	0.17	0.13	0.13
T (magnitude)	0.08	0.04	0.08

Standard errors are shown in parentheses. For location and release time, only the typical magnitude (standard deviation across possible values) is shown. Outcome parameters are IA (impact area, in m^2), IR (impact range, in m), and DT (dissolution time, in s).

used (Lovdata, 2019). A buffer zone of 500 m offers a good level of protection from releases having a toxicity threshold of 10% but is less effective when the toxicity threshold is 1% or smaller.

Chemical releases in sheltered areas within fjords appear to have wider impact ranges, larger impact zones, and longer dissolution times compared to more exposed areas off the coast. Ocean masses within fjords are often strongly stratified, which inhibits vertical mixing and leads to slower dissolution rates. In addition, freshwater runoff from rivers can create a persistent fjord outflow in the upper layers, which may transport the plume further away without dissolving it. The mean effect of location is moderate compared to the importance of the toxicity threshold. Still, the difference between the most sheltered and most exposed location in our dataset is comparable to the difference between $C = 0.001$ and $C = 0.01$.

The mean impact area, dissolution time, and impact range are all peaking during the summer season. This is expected as stratification is stronger in the summer, especially in the fjords, due to increased freshwater runoff and elevated surface temperatures. The overall effect is not as large as the location effect, but there might be specific locations where the seasonal effect is more pronounced.

Location and local current speed are correlated but give independent contributions to the outcome parameters. While strong currents may transport the plume faster, it often leads to increased turbulent mixing and rapid dissolution. It seems like these effects cancel out when it comes to impact area, leaving only a weak correlation. The effect of current speed on impact range and dissolution time is stronger, but not as important as location.

Implications for policymakers

Our results demonstrate that chemicals released from tarpaulin bath treatments can affect large areas far from the release point. Factors that strongly influence the damage potential are the release volume and the harmful concentration relative to the release concentration. Policymakers may want to consider restrictions on bath treatment activity that occur close to sensitive habitats, especially if the active chemical is harmful at small concentrations. Restrictions may include banning the use of certain chemicals, capping the permissible release volume or restricting the number of allowed tarpaulin operations per year. Bath treatments may alternatively be performed using wellboats where the wastewater is released gradually while the boat is moving, contributing to rapid dilution of the chemicals (Refseth *et al.*, 2019). With wellboats, the treatment water can also be transported away from sensitive habitats before being released.

Even if the release volume and type of chemical is fixed, the impact range varies considerably. This is primarily due to variations

Downloaded from https://academic.oup.com/icesjms/article/79/1/22/6453070 by Institute of Marine Research user on 17 February 2022

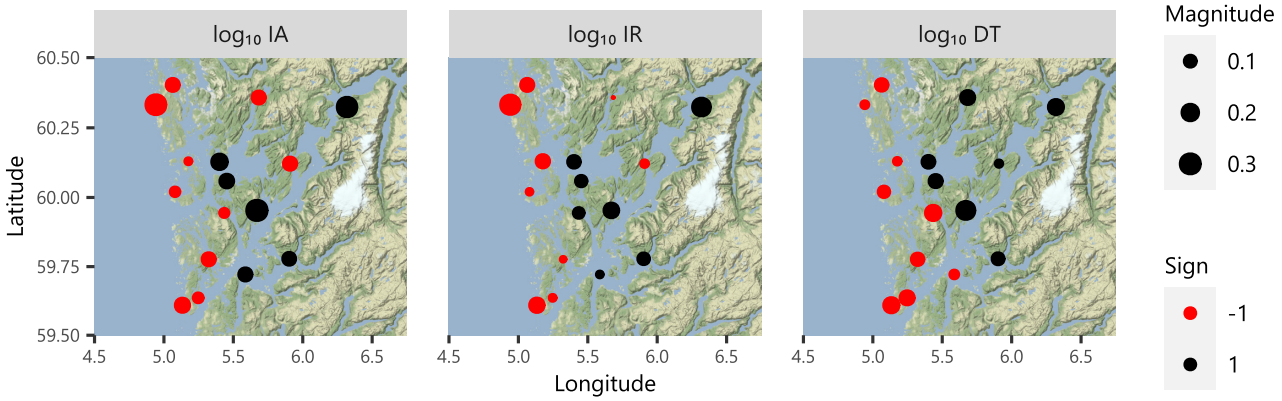

Figure 3. Effect of location on impact area (*IA*), impact range (*IR*), and dissolution time (*DT*) according to the model defined by Equation (2).

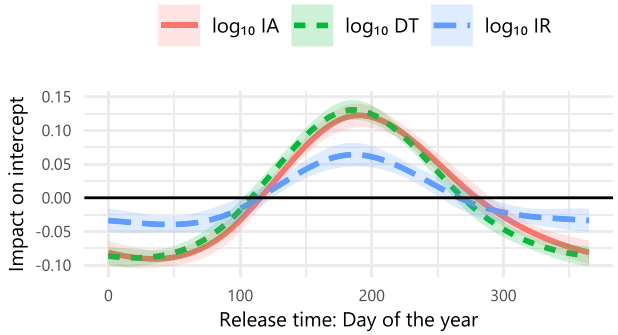

Figure 4. Effect of release time on impact area (IA), impact range (IR), and dissolution time (DT) according to the model defined by Equation (2). Shaded bands denote 95% confidence intervals.

in the current patterns in the wider region around the release point. On average, some locations give larger impact ranges than others, but the variation within each location is usually greater than the difference between them. The large amount of variation makes it difficult to define an absolute "safety distance" from the release point, beyond which no harmful effects can be expected. Instead, there is a wide region around the farm where harmful exposure is unlikely, but not impossible. Policy makers will have to decide whether this risk is acceptable or not.

Sample application: kelp forests

Below, we apply our statistical results to assess the harmful potential of a hydrogen peroxide release on nearby populations of sugar kelp (*Saccharina latissima*). We consider a tarpaulin operation where 18000 m^3 of treatment water is released, with a treatment concentration of 1500 mg/L and a local current speed at 5 m depth of $U = 0.1$ m/s.

The LC_{50} of juvenile sugar kelp at 1 hour exposure to H_2O_2 was estimated by Haugland *et al.* (2019) to be 81 mg/L, which is 0.054 times the release concentration. Scaling by the release volume, this equals a toxicity threshold of $C = 0.048$, which is halfway between our reference thresholds of 0.1 and 0.01. Interpolating on a log scale as described in the methods section, we get $\beta_C^{[0.1]} = 0.68$ and $\beta_C^{[0.001]} = 0$. From Equation (2), we predict a $\log_{10}$ impact range of 2.68 ± 0.24 (mean $\pm$ *SD*), i.e. an interval of 275 m–831 m. This interval represents the most probable impact range, but shorter and longer impact ranges are also possible.

If the location is known to be a sheltered fjord location, we can set $\beta_L = 0.13$ (1 *SD*, Table 4), which raises the predicted impact range by 35%. Conversely, if the location is known to be highly exposed, we can set $\beta_L = -0.13$, which reduces the impact range to 74% of the original.

Next, assume that we are interested in a specific kelp forest located 900 m from the release point. The probability that the plume will reach this location is 1.0 % according to our statistical model. If there are 100 kelp forests at 900 m distance from the farm, it is expected that one of these are exposed to harmful concentrations after the release. Note that this probability does not take vertical distribution into account. The plume is most likely to stay in the upper 10–20 m of the water column. Some of the kelp may be growing at depths of 20–30 m, and the probability of exposure to these areas is smaller.

The $\log_{10}$ impact area is estimated to 5.04 ± 0.23 (mean $\pm$ *SD*), which equals an interval of 0.06 km^2–0.19 km^2. This is an upper limit to the amount of kelp that can be exposed to harmful concentrations by a single release, which is only attained if the plume is released in the middle of a kelp forest.

The predicted dissolution time is 1.0 hr–2.4 hr (mean $\pm$ *SD*). It is recommended that no additional releases are performed within this time period. Otherwise, the concentration of the new release is added to the remaining concentration of the old release, which slows down dilution and increases the impact area and range. Plume dissolution time is not directly related to the exposure time for individual kelp plants, which is potentially much shorter than the time it takes to dissolve the plume completely.

All numbers presented above are based on the LC_{50} value. Another relevant endpoint is the EC_{50} value of 28 mg/L (Haugland *et al.*, 2019), which includes sub-lethal effects of reduced photosynthetic capacity and efficiency. Assuming unchanged treatment volume of 18000 m^3 and treatment concentration of 1500 mg/L, the toxicity threshold drops from 0.048 to 0.014 by using this endpoint. This increases the mean impact range from 480 m to 1200 m, and the mean impact area from 0.11 km^2 to 0.45 km^2. Similarly, the impact range and area increase if the treatment concentration or treatment volume is increased.

Downloaded from https://academic.oup.com/icesjms/article/79/1/22/6453070 by Institute of Marine Research user on 17 February 2022

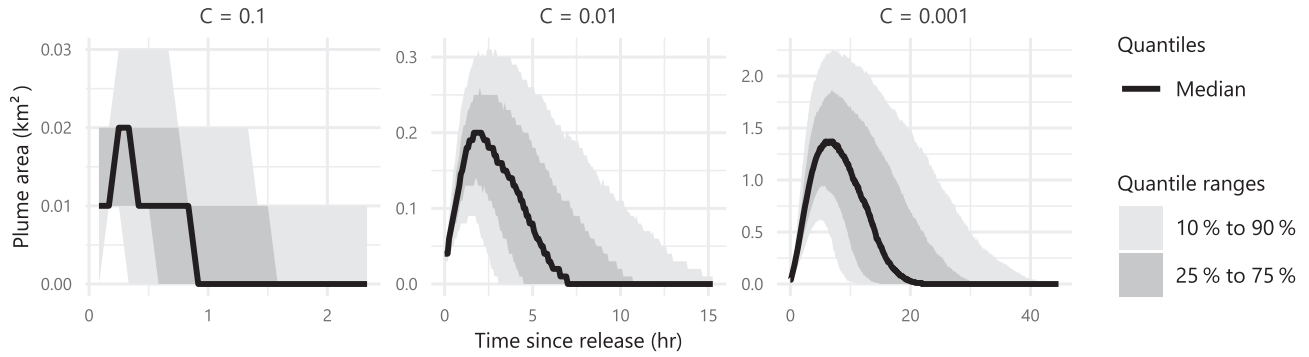

Figure 5. Instantaneous area of the plume at different points in time for all simulations, grouped by toxicity threshold (*C*). Note the different spatial and temporal scales.

Table 5. Coefficients for the regression model in Equation (3), which estimates exposure probability (*EP*).

Covariate	logit *EP*
(Intercept)	−0.41
C [0.001]	0.83
C [0.1]	−0.93
U	−1.83
L (magnitude)	0.38
T (magnitude)	0.40
D	−1.55
D × *C*[0.001]	0.79
D × *C*[0.1]	−3.34
D × *U*	0.52
D × *L* (magnitude)	0.85
D × *T* (magnitude)	0.10

Covariates in the table are *D* (distance from release location, in km), *U* (ocean current speed at 5 m depth, in m/s), *C* (toxicity threshold), *L* (location, 16 levels), and *T* (time, 4-knot cyclic spline). For location and release time, only the typical magnitude (standard deviation across possible values) is shown.

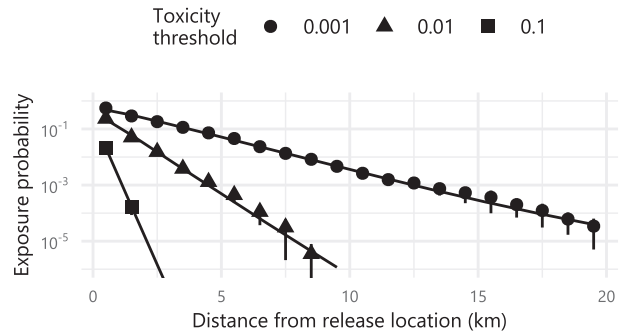

Figure 6. Probability of being exposed to harmful concentration at a certain distance from the release point. Markers represent the mean probability from simulations, across all farms and release times. Vertical lines represent the 95 % confidence interval of the mean. Sloped lines represent the regression mean as defined by Equation (3).

Comparison with previous works

Refseth *et al.* (2019) performed simulations of hydrogen peroxide releases from four Norwegian fish farm locations, using a treatment volume of 21000 m^3 and a treatment dose of 2000 mg/L. A toxicity threshold of 0.01 in our simulations thus corresponds to a field concentration of 26.25 mg/L in their simulations. Visual inspection of the provided figures suggests that the impact range of their simulations are similar to ours, but a direct comparison is difficult since they only report the largest observed concentration over a course of 48 individual release times. The report states that concentrations of 10 mg/L can occur ∼5 km from the release, which fits well with our own data.

Ernst *et al.* (2014) performed field measurements of azamethiphos and deltamethrin after six separate operational tarpaulin bath treatments in New Brunswick, Canada. Fluorescent dye was added to track the wastewater plume. The treatment volume was 800 m^3, which is 0.05 times the reference volume of 16000 m^3 used in our simulations. A toxicity threshold of 0.1 in our dataset therefore corresponds to a dilution of 1:200 in their field study. The plumes tracked in their study reached this dilution level within 150 m to 1700 m from the release site. Our data suggest an impact range of 160 m–430 m at this toxicity threshold (25%–75 % percentile), with a maximal value of 2 km. Thus their measurements agree with our simulations. One should also take into account that their field samples are point measurements taken in the middle of the plume, while our model data represent the average concentration within computational cells of 100 m × 100 m. It is therefore not surprising that their measurements are somewhat at the high end of the scale compared with the simulations.

Model limitations

The main limitation to the simulation model is that released chemicals are assumed to follow the currents passively. This may give misleading results for hydrogen peroxide if the water column is well-mixed, since the plume may sink downwards due to its density (Refseth *et al.*, 2019). Also, in a strongly stratified water column, the well-mixed treatment water may migrate into a narrow vertical layer upon tarpaulin release. Neither of these effects are included in the particle tracking model, and future research is required to quantify them. Another effect not included in the model is additional dispersion and drift due to surface waves. We do not expect this to be a significant source of error, but large wave activity may improve the plume dilution rate somewhat. Tarpaulin operations are mostly performed when the wave height is small, due to technical considerations.

Our model does not currently include the vertical and horizontal migration behaviour of non-target species. Impact assessments must take this behaviour into account as well. For instance,

Downloaded from https://academic.oup.com/icesjms/article/79/1/22/6453070 by Institute of Marine Research user on 17 February 2022

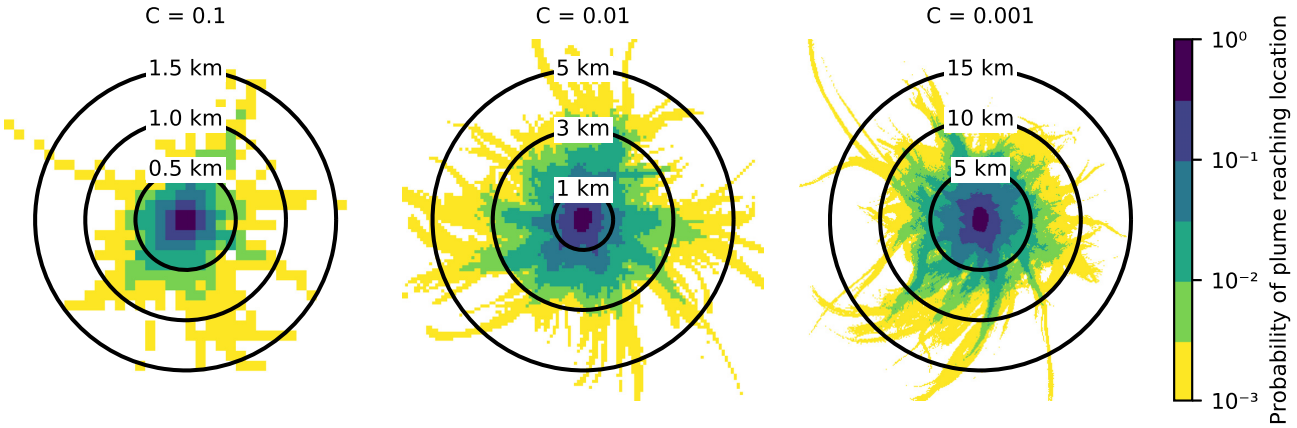

Figure 7. Overlay of exposure areas for all release times and locations, grouped by toxicity threshold (C). Note the different length scale in each subfigure. Colours indicate the fraction of releases exceeding the toxicity threshold.

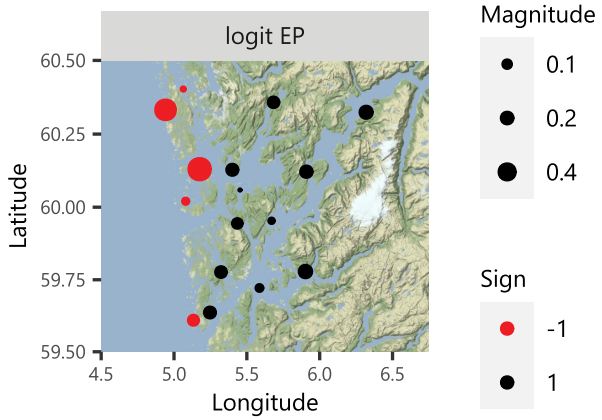

Figure 8. Impact of location times distance on exposure probability, as estimated by the regression model in Equation (3). The magnitude must be interpreted using the logit link of the regression model.

deep-dwelling species are less likely to encounter neutrally buoyant plumes, which will mostly stay in the upper layers of the water column. Zooplankton often have a diurnal vertical migration cycle, which gives a higher probability of exposure during night-time (Stich and Lampert, 1981; Lampert, 1989; Heywood, 1996). Horizontal migration behaviour may influence both the exposure probability and the exposure time. Organisms who follow the ocean currents passively stay in the same body of water for a long time and are less likely to encounter a nearby plume than stationary or upstream-swimming species. On the other hand, if a passively transported organism does get mixed into the plume, it is likely to stay in the plume for a longer time. One should also note that few organisms are truly passive drifters in the vertical direction. For instance, buoyant and upwards-swimming plankton may be temporarily captured by local convergence zones (Skarðhamar *et al.*, 2007; Mann and Lazier, 2013). This increases the chance of exposure to nearby plumes passing through the convergence zone.

Degradation of the released substances is not included in the model. The mechanisms behind degradation are manifold, depending on the chemical in question. For instance, hydrogen peroxide is an oxidising agent, which may react with organic substances in the seawater, catalysed by light and various planktonic species (Wong *et al.*, 2003). The reported half-life varies wildly in the literature, most are in the order of days or weeks while some are in the order of hours [see Lyons *et al.* (2014) and the references therein]. The half-life of deltamethrin is estimated to 18 hours in the aqueous phase (Erstfeld, 1999), but the chemical is also strongly lipophilic and attaches to particles, sediment, and organisms (Ernst *et al.*, 2014), thus removing it from the water phase. Azamethiphos is water soluble and more stable, with a half-life in the order of ~10 days (Worthing and Walker, 1987). In general, any degradation process that happen on time scales comparable to the dissolution time will reduce the impact range, area, and dissolution time. For most applications, dispersion by hydrodynamic currents is still expected to be the dominant effect.

In our simulations, we assume that the ocean is pristine at the time of the release. In practice, cages are often treated successively, with pulses of chemicals released repeatedly into the ocean. Multiple exposures have the potential of being harmful to sensitive organisms even if the chemical is highly diluted (Bechmann *et al.*, 2019).

Conclusions and further work

We have performed high-resolution simulations of chemical releases from fish farms and summarized the results in a statistical regression model. Four parameters quantifying the damage potential were estimated: the impact area, impact range, dissolution time, and exposure probability. The main variable controlling all of these parameters is the toxicity threshold, which is the amount of large-scale dilution required to neutralize the released chemical, scaled by the release volume [Equation (1)]. If the released volume is large and the wastewater is highly toxic, harmful concentrations are found over 20 km from the release point in rare instances. At exposed locations, plumes dissolve faster, and the average impact area and range are smaller. Still, the difference between locations were smaller than the variation within locations. Seasonal differences were statistically significant, but smaller than the effect of location.

Further research may be directed at quantifying the exposure probability of specific species by coupling the plume drift model to a biological model of chemical sensitivity and vertical/horizontal migration, possibly including chemical degradation. Further research may also be directed at estimating impact zones for well boat releases. An additional topic for further study is the effect of ocean stratification and wastewater density on the initial plume distribu-

Downloaded from https://academic.oup.com/icesjms/article/79/1/22/6453070 by Institute of Marine Research user on 17 February 2022

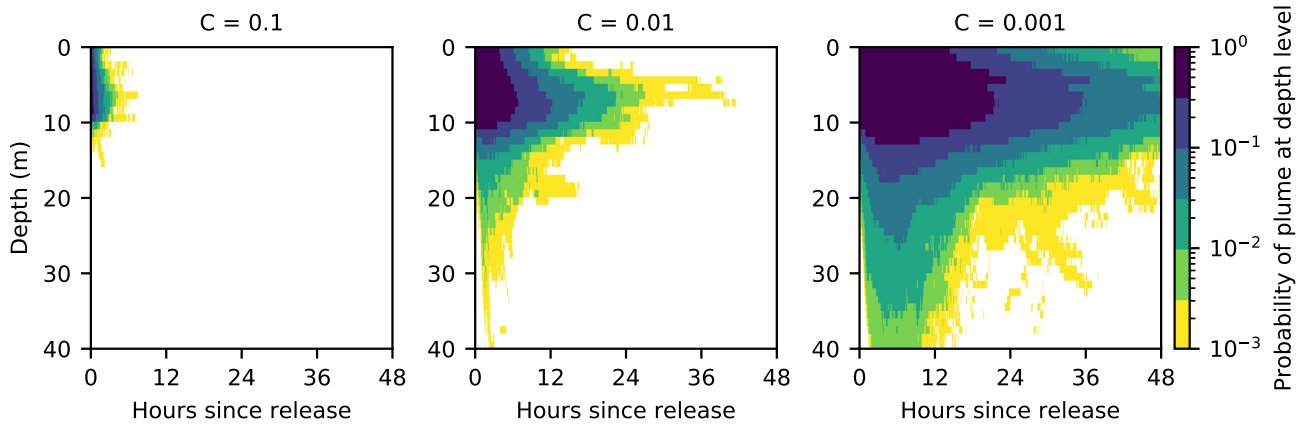

Figure 9. Overlay of plume vertical distributions as a function of time, for all release times and locations, grouped by the toxicity threshold (*C*). Colours indicate the fraction of simulated wastewater plumes reaching the indicated depth.

tion, which is not studied in this paper. One may also consider a broader geographical range of release sites. Simulations from multiple years could be useful to study interannual variations.

Data availability

The model data underlying this article will be shared on reasonable request to the corresponding author.

References

Albretsen, J., Sperrevik, A. K., Staalstrøm, A., Sandvik, A. D., Vikebø, F., and Asplin, L. 2011. NorKyst-800 Report No. 1: User Manual and Technical Descriptions. 2–2011. Fisken Og Havet.. Institute of Marine Research.

Andersen, P. A., and Hagen, L. 2016. Fortynningsstudier: Hydrogenperoksid. 156-8–16. Aqua Kompetanse AS.

Arakawa, A., and Lamb, V. R. 1977. Computational design of the basic dynamical processes of the UCLA general circulation model. In Methods in Computational Physics: Advances in Research and Applications, pp. 174–267. Academic Press, New York.

Asplin, L., Albretsen, J., Johnsen, I.A., and Sandvik, A. D. 2020. The hydrodynamic foundation for salmon lice dispersion modeling along the Norwegian coast. Ocean Dynamics, 70: 1151–1167. https://doi.org/10.1007/s10236-020-01378-0.

Asplin, L., Johnsen, I. A., Sandvik, A. D., Albretsen, J., Sundfjord, V., Aure, J., and Boxaspen, K. K. 2014. Dispersion of salmon lice in the Hardangerfjord. Marine Biology Research, 10: 216–225. https://doi.org/10.1080/17451000.2013.810755.

Bechmann, R. K., Arnberg, M., Gomiero, A., Westerlund, S., Lyng, E., Berry, M., Agustsson, T. *et al.* 2019. Gill damage and delayed mortality of northern shrimp (*Pandalus borealis*) after short time exposure to anti-parasitic veterinary medicine containing hydrogen peroxide. Ecotoxicology and Environmental Safety, 180: 473–482. https://doi.org/10.1016/j.ecoenv.2019.05.045.

Bergh, Ø. 2007. The dual myths of the healthy wild fish and the unhealthy farmed fish. Diseases of Aquatic Organisms, 75: 159–164. https://doi.org/10.3354/dao075159.

Brokke, K. E. 2015. Mortality Caused by De-Licing Agents on the Non-Target Organisms Chameleon Shrimp (*Praunus flexuosus*) and Grass Prawns (*Palaemon elegans*). Department of Biology, University of Bergen.

Costello, M. J. 2009. The global economic cost of sea lice to the salmonid farming industry. Journal of Fish Diseases, 32: 115–118. https://doi.org/10.1111/j.1365-2761.2008.01011.x.

Dalsøren, S. B., Albretsen, J., and Asplin, L. 2020. New validation method for hydrodynamic fjord models applied in the Hardangerfjord, Norway. Estuarine, Coastal and Shelf Science, 246: 107028. https://doi.org/10.1016/j.ecss.2020.107028.

Döös, K., Kjellsson, J., and Jönsson, B. 2013. TRACMASS—a Lagrangian trajectory model. In Preventive Methods for Coastal Protection: Towards the Use of Ocean Dynamics for Pollution Control, pp. 225–249. Ed. by Soomere, Tand and Quak, T. Springer International Publishing, Heidelberg. https://doi.org/10.1007/978-3-319-00440-2_7.

Ernst, W., Doe, K., Cook, A., Burridge, L., Lalonde, B., Jackman, P., Aubé, J. G. *et al.* 2014. Dispersion and toxicity to non-target crustaceans of azamethiphos and deltamethrin after sea lice treatments on farmed salmon, *Salmo salar*. Aquaculture, 424-425: 104–112. https://doi.org/10.1016/j.aquaculture.2013.12.017.

Erstfeld, K. M. 1999. Environmental fate of synthetic pyrethroids during spray drift and field runoff treatments in aquatic microcosms. Chemosphere, 39: 1737–1769. https://doi.org/10.1016/S0045-6535(99)00064-8.

Escobar-Lux, R. H., Fields, D. M., Browman, H. I., Shema, S. D., Bjelland, R. M., Agnalt, A-L., Skiftesvik, A. *et al.* 2019. The effects of hydrogen peroxide on mortality, escape response and oxygen consumption of Calanus spp. FACETS, 4, 626–637. https://doi.org/10.1139/facets-2019-0011.

Escobar-Lux, R. H., and Samuelsen, O. B. 2020. The acute and delayed mortality of the Northern krill (*Meganyctiphanes norvegica*) when exposed to hydrogen peroxide. Bulletin of Environmental Contamination and Toxicology, 105: 705–710. https://doi.org/10.1007/s00128-020-02996-6.

Fagereng, M. B. 2016. Bruk av hydrogenperoksid i oppdrettsanlegg; fortynningstudier og effekter på blomsterreke (*Pandalus montagui*). Master thesis. https://bora.uib.no/handle/1956/13008.

Fang, J., Samuelsen, O. B., Strand, Ø., and Jansen, H. 2018. Acute toxic effects of hydrogen peroxide, used for salmon lice treatment, on the survival of polychaetes *Capitella* sp. and *Ophryotrocha* spp. Aquaculture Environment Interactions, 10: 363–368. https://doi.org/10.3354/aei00273.

FAO. 2020. Global Aquaculture Production. 2020. http://www.fao.org/fishery/statistics/global-aquaculture-production/en, Last accessed: April 1th 2021.

Forseth, T., Barlaup, B. T., Finstad, B., Fiske, P., Gjøsæter, H., Falkegård, M., Hindar, A. *et al.* 2017. The major threats to Atlantic salmon in Norway. ICES Journal of Marine Science, 74: 1496–1513. https://doi.org/10.1093/icesjms/fsx020.

Gräwe, U. 2011. Implementation of high-order particle-tracking schemes in a water column model. Ocean Modelling, 36: 80–89. https://doi.org/10.1016/j.ocemod.2010.10.002.

Hamilton-West, C., Arriagada, G., Yatabe, T., Valdés, P., Hervé-Claude, L. P., and Urcelay, S. 2012. Epidemiological description of the sea lice (*Caligus rogercresseyi*) situation in southern Chile in August 2007.

Downloaded from https://academic.oup.com/icesjms/article/79/1/22/6453070 by Institute of Marine Research user on 17 February 2022

Preventive Veterinary Medicine, 104: 341–345. https://doi.org/10.1016/j.prevetmed.2011.12.002.

Haugland, B. T., Rastrick, S. P. S., Agnalt, A-L., Husa, V., Kutti, T., and Samuelsen, O. B. 2019. Mortality and reduced photosynthetic performance in sugar kelp Saccharina latissima caused by the salmon-lice therapeutant hydrogen peroxide. Aquaculture Environment Interactions, 11: 1–17. https://doi.org/10.3354/aei00292.

Heuch, Pa, and Mo, Ta. 2001. A model of salmon louse production in Norway: effects of increasing salmon production and public management measures. Diseases of Aquatic Organisms, 45: 145–152. https://doi.org/10.3354/dao045145.

Heywood, K. J. 1996. Diel vertical migration of zooplankton in the northeast Atlantic. Journal of Plankton Research, 18: 163–184. https://doi.org/10.1093/plankt/18.2.163.

Hunter, J. D. 2007. Matplotlib: a 2D graphics environment. Computing in Science & Engineering, 9: 90–95. https://doi.org/10.1109/MCSE.2007.55.

Hvidsten, N. A., Finstad, B., Kroglund, F., Johnsen, B. O., Strand, R., Arnekleiv, J. V., and Bjørn, P. A. 2007. Does increased abundance of sea lice influence survival of wild Atlantic salmon post-smolt? Journal of Fish Biology, 71: 1639–1648. https://doi.org/10.1111/j.1095-8649.2007.01622.x.

Jansen, B. C. B. 2018. Felleskatalogen over Farmasøytiske Preparater Markedsført i Norge Til Bruk i Veterinærmedisinen 2018-2019. Felleskatalogen.Oslo, Norway

Johnsen, Ia, Fiksen, ø, Sandvik, Ad, and Asplin, L. 2014. Vertical salmon lice behaviour as a response to environmental conditions and its influence on regional dispersion in a fjord system. Aquaculture Environment Interactions, 5: 127–141. https://doi.org/10.3354/aei00098.

Johnsen, I. A., Harvey, A., Sævik, P. N., Sandvik, A. D., Ugedal, O., Ådlandsvik, B., Wennevik, V. *et al.* 2020. Salmon lice-induced mortality of Atlantic salmon during post-smolt migration in Norway. ICES Journal of Marine Science, 78: 142–154. https://doi.org/10.1093/icesjms/fsaa202.

Johnson, S. C., Bravo, S., Nagasawa, K., Kabata, Z., Hwang, J., Ho, J., and Shih, C. T. 2004. A review of the impact of parasitic copepods on marine aquaculture. Zoological Studies, 43: 229–243.

Kabata, Z. 1974. Lepeophtheirus cuneifer sp. nov. (Copepoda: Caligidae), a parasite of fishes from the Pacific coast of North America. Journal of the Fisheries Research Board of Canada, 31: 43–47. https://doi.org/10.1139/f74-006.

Kahle, D., and Wickham, H. 2013. Ggmap: spatial visualization with Ggplot2. The R Journal, 5: 144. https://doi.org/10.32614/RJ-2013-014.

Kantha, L. H., and Clayson, C. A. 2000. Numerical Models of Oceans and Oceanic Processes. Academic Press, San Diego.

Kragesteen, T. J., Simonsen, K., Visser, A. W., and Andersen, K. H. 2019. Optimal salmon lice treatment threshold and tragedy of the commons in salmon farm networks. Aquaculture, 512: 734329. https://doi.org/10.1016/j.aquaculture.2019.734329.

LaBolle, E. M., Quastel, J., Fogg, G. E., and Gravner, J. 2000. Diffusion processes in composite porous media and their numerical integration by random walks: Generalized stochastic differential equations with discontinuous coefficients. Water Resources Research, 36: 651–662. https://doi.org/10.1029/1999WR900224.

Lampert, W. 1989. The adaptive significance of diel vertical migration of zooplankton. Functional Ecology, 3: 21–27. https://doi.org/10.2307/2389671.

Lovdata. 2018. Forskrift om bekjempelse av lakselus i akvakulturanlegg (FOR-2012-12-05-1140). https://lovdata.no/dokument/SF/forskrift/2012-12-05-1140, Last accessed: April 1th, 2021.

Lovdata. 2019. Forskrift om drift av akvakulturanlegg (FOR-2008-06-17-822). 2019. https://lovdata.no/dokument/SF/forskrift/2008-06-17-822.

Lyons, M. C., Wong, D. K. H., and Page, F. H. 2014. Degradation of Hydrogen Peroxide in Seawater Using the Anti-Sea Louse Formulation Interox Paramove 50. Fisheries and Oceans Canada, Maritimes Region, St. Andrews Biological Station, St. Andrews, NB.

Mann, K. H., and Lazier, J. R. N. 2013. Dynamics of Marine Ecosystems: Biological-Physical Interactions in the Oceans. John Wiley & Sons.Hoboken, NJ

Müller, M., Homleid, M., Ivarsson, K-I., Køltzow, M. A. Ø., Lindskog, M., Midtbø, K. H., Andrae, U. *et al.* 2017. AROME-MetCoOp: a Nordic convective scale operational weather prediction model. Weather and Forecasting, 32: 609–627. https://doi.org/10.1175/WAF-D-16-0099.1.

Parsons, A. E., Escobar-Lux, R. H., Sævik, P. N., Samuelsen, O. B., and Agnalt, A-L. 2020. The impact of anti-sea lice pesticides, azamethiphos and deltamethrin, on European lobster (*Homarus gammarus*) larvae in the Norwegian marine environment. Environmental Pollution, 264: 114725. https://doi.org/10.1016/j.envpol.2020.114725.

Refseth, G. H., Nøst, O. A., Evenset, A., Tassara, L., Espenes, H., Drivdal, M., Augustin, S. *et al.* 2019. Risk assessment and risk reducing measures for discharges of hydrogen peroxide (H2O2). 8948–1. Akvaplan-niva AS. https://www.fhf.no/prosjekter/prosjektbasen/901416/. Last accessed: April 1th, 2021.

Refseth, G. H., Sæther, K., Drivdal, M., Nøst, O. A., Augustine, S., Camus, L., Tassara, L. *et al.* 2016. Miljørisiko Ved Bruk Av Hydrogenperoksid. Økotoksikologisk Vurdering Og Grenseverdi for Effekt. 8200. Akvaplan-niva. Last accessed: April 1th, 2021.

R Studio Team. 2019. RStudio: Integrated Development Environment for R (version 1.2.5019). Rstudio, Inc, Boston, MA. http://www.rstudio.com/. Last accessed: April 1th, 2021.

Rudiger, P., Stevens, J-L., Bednar, J. A., Nijholt, B., Andrew, C. B., Randelhoff, A. *et al.* 2020. Holoviz/Holoviews: version 1.13.3. Zenodo. https://doi.org/10.5281/ZENODO.3904606.

Shchepetkin, A. F., and McWilliams, J. C. 2005. The regional oceanic modeling system (ROMS): a split-explicit, free-surface, topography-following-coordinate oceanic model. Ocean Modelling, 9: 347–404. https://doi.org/10.1016/j.ocemod.2004.08.002.

Skaala, Ø., Kålås, S., and Borgstrøm, R. 2014. Evidence of salmon lice-induced mortality of anadromous brown trout (*Salmo trutta*) in the Hardangerfjord, Norway. Marine Biology Research, 10: 279–288. https://doi.org/10.1080/17451000.2013.810756.

Skarðhamar, J., Slagstad, D., and Edvardsen, A. 2007. Plankton distributions related to hydrography and circulation dynamics on a narrow continental shelf off Northern Norway. Estuarine, Coastal and Shelf Science, 75: 381–392. https://doi.org/10.1016/j.ecss.2007.05.044.

Smagorinsky, J. 1963. General circulation experiments with the primitive equations: I. The basic experiment. Monthly Weather Review, 91: 99–164. https://doi.org/10.1175/1520-0493(1963)091⟨0099:GCEWTP⟩2.3.CO;2.

Stich, H-B., and Lampert, W. 1981. Predator evasion as an explanation of diurnal vertical migration by zooplankton. Nature, 293: 396–398. https://doi.org/10.1038/293396a0.

Taranger, G. L., Karlsen, Ø., Bannister, R. J., Glover, K. A., Husa, V., Karlsbakk, E., Kvamme, B. O. *et al.* 2015. Risk assessment of the environmental impact of Norwegian Atlantic salmon farming. ICES Journal of Marine Science, 72: 997–1021. https://doi.org/10.1093/icesjms/fsu132.

Torrissen, O., Jones, S., Asche, F., Guttormsen, A., Skilbrei, O. T., Nilsen, F., Horsberg, T. E., and Jackson, D. 2013. Salmon lice - impact on wild salmonids and salmon aquaculture. Journal of Fish Diseases, 36: 171–194. https://doi.org/10.1111/jfd.12061.

Umlauf, L., and Burchard, H. 2003. A generic length-scale equation for geophysical turbulence models. Journal of Marine Research, 61: 235–265. https://doi.org/10.1357/002224003322005087.

Urbina, M. A., Cumillaf, J. P., Paschke, K., and Gebauer, P. 2019. Effects of pharmaceuticals used to treat salmon lice on non-target species: evidence from a systematic review. Science of The Total Environment, 649: 1124–1136. https://doi.org/10.1016/j.scitotenv.2018.08.334.

Volent, Z., Birkevold, J., Stahl, A., Lien, A., Sunde, L. M., and Lader, P. 2017. Experimental study of installation procedure and volume estimation of tarpaulin for chemical treatment of fish in floating

Downloaded from https://academic.oup.com/icesjms/article/79/1/22/6453070 by Institute of Marine Research user on 17 February 2022

cages. Aquacultural Engineering, 78: 105–113. https://doi.org/10.1016/j.aquaeng.2017.05.003.
Wickham, H. 2016. Ggplot2: Elegant Graphics for Data Analysis, 2nd edn. Springer-Verlag, New York.
Wong, G. T. F., Dunstan, W. M., and Kim, D-B. 2003. The decomposition of hydrogen peroxide by marine phytoplankton. Oceanologica Acta, 26: 191–198. https://doi.org/10.1016/S0399-1784(02)00006-3.
Wootten, R., Smith, J. W., and Needham, E. A. 1982. Aspects of the biology of the parasitic copepods *Lepeophtheirus salmonis* and *Caligus elongatus* on farmed salmonids, and their treatment. Proceedings of the Royal Society of Edinburgh. Section B. Biological Sciences, 81: 185–197. https://doi.org/10.1017/S0269727000003389.
Worthing, C. R., and Walker, S. B. (Ed.). 1987. The Pesticide Manual: A World Compendium. 8th edn. British Crop Protection Council, Farnham, Surrey.

Handling Editor: Carrie Byron

Downloaded from https://academic.oup.com/icesjms/article/79/1/22/6453070 by Institute of Marine Research user on 17 February 2022